Recent airborne remote sensing applications in Svalbard

Shridhar D. Jawak 1, Emiliana Valentini 2, Agnar Sivertsen 3, Trond Løke 4, Friederike Körting 4, Na Liu 4, Achut Parajuli 5, Esther Mas Sanz 6, Joanna Szafraniec 7, Julian Podgorski 8, Marie Henriksen 9, Oliver Hasler 9, Sagar Wankhede 10, Shunan Feng11, Riccardo Cerrato 2, Ximena A. Vega 12, Aleksandra Osika7, Benjamin A. Lange 13, William D. Harcourt 14, Christiane Hübner 1, Inger Jennings 1, Dariusz Ignatiuk 7, Ilkka Matero 1, Øystein Godøy1 and Heikki Lihavainen 1.

1Svalbard Integrated Arctic Earth Observing System (SIOS), SIOS Knowledge Centre (SIOS-KC), Post Box 156, Svalbard Science Centre, 9170 Longyearbyen, Svalbard, Norway; shridhar.jawak@sios-svalbard.org
2CNR - Consiglio Nazionale delle Ricerche, Italy; emiliana.valentini@cnr.it 3NORCE Norwegian Research Centre, Tromsø, Norway; agsi@norceresearch.no 4Norsk Elektro Optikk AS, Østensjøveien 34, 0667 Oslo, Norway; trond@neo.no
5 University of Quebec at Trois Rivieres, Canada; Achut.Parajuli@uqtr.ca 6DTU - Technical University of Denmark; esther.mas.96@gmail.com 7 University of Silesia in Katowice; joanna.szafraniec@us.edu.pl
8Institute of Geophysics, Polish Academy of Sciences; jpodgo@igf.edu.pl 9Norwegian University of Science and Technology; marie.b.henriksen@ntnu.no; oliver.hasler@ntnu.no 10 Dept. of Civil Engineering, Manipal Institute of Technology, Manipal Academy of Higher Education, Manipal 576104, Karnataka, India; sagar.wankhede@learner.manipal.edu 11Aarhus University, Denmark; shunan.feng@envs.au.dk 12University of Stirling, U.K; x.a.aguilar.vega@stir.ac.uk
13Norwegian Polar Institute, Norway; Benjamin.Lange@npolar.no 14University of St Andrews, UK; wdh1@st-andrews.ac.uk

Introduction

- The Svalbard Integrated Arctic Earth Observing System (SIOS) support airborne remote sensing (RS) platforms to complement in situ observations and to reduce the environmental footprint of science.
- SIOS member institution Norwegian Research Centre (NORCE) mounted sensors on the Lufttransport Dornier aircraft as part of the SIOS-InfraNor project. The Dornier aircraft acquires RGB imagery and hyperspectral data.
- SIOS has supported 20 scientific projects to acquire data in Svalbard using this aircraft. Identifying glacier crevasses, generating digital elevation models (DEMs), mapping and characterising minerals, vegetation, and seasonal changes in sea ice, snow cover, and ocean colour are a few applications.
- In September 2021, SIOS hosted a training course on hyperspectral RS using airborne imaging sensor data. This study presents two examples from this course to demonstrate the potential of airborne imaging sensors in Svalbard.

Methods

Two types of hyperspectral datasets were used.

DORNIER (1)

- **spatial resolution**: 1m/pixel
- **spectral resolution**: 186 bands (400 - 1000 nm)

PRISMA (2)

- **spatial resolution**: 30 m VNIR/SWIR 5 m PAN.
- **spectral range**: 400 – 1010 nm VNIR 920 – 2505 nm SWIR 400 – 700 nm for PAN.
- 239 bands (66 VNIR and 173 SWIR).

(1) Acquisition over area 1 (fig. 1) on 28th August 2021.

(2) Level 2D images (atmospherically and geometrically corrected) (1) Krossfjorden (2) Barentsburg (3) Polarisbreen (fig. 1).

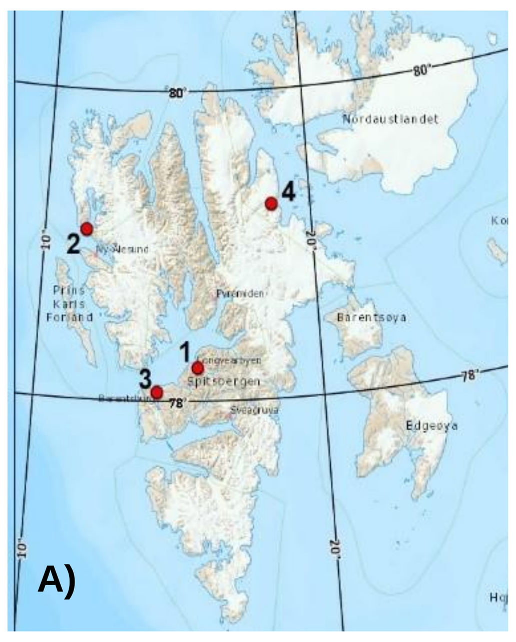

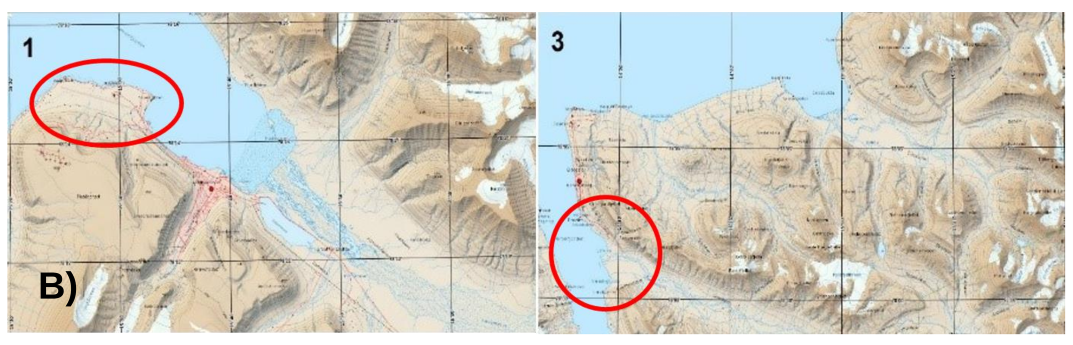

Figure 1: Study areas in Svalbard (A) (1) Adventdalen, Longyearbyen, (2) Kongsfjord, NyÅlesund (3), Barentsburg, and (4) Polarisbreen, Ursafonna in Ny Friesland, NE Spitsbergen. Examples presented in this study (B).

- **Processing and analysis**

(1) DORNIER

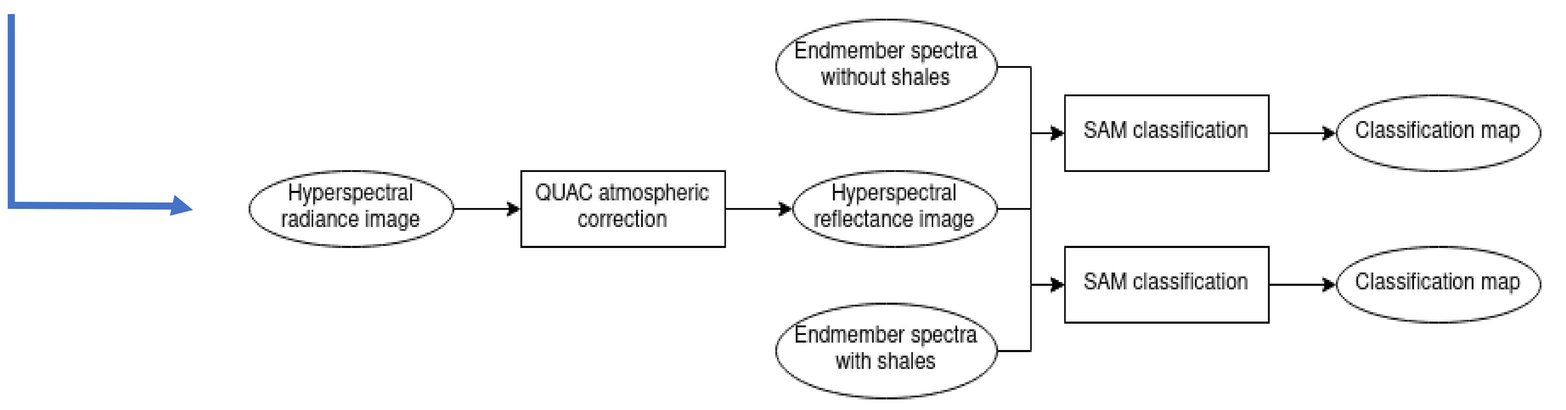

(2) PRISMA

Pre-processing:

1. Mask NaN values
2. Denoise image
3. Cloud mask – Water mask
4. Apply indexes (fig. 3)

- NDVI (normalized difference vegetation index) [1]
  - With R_RED = 679 nm and R_NIR = 699 nm
  $$NDVI = \frac{R_{NIR} - R_{RED}}{R_{NIR} + R_{RED}}$$
- FLH (fluorescence line height) [2]
  - With b1 = 660 nm, b2 = 679 nm and b3 = 729 nm
  $$FLH = b_2 - b_3 + (b_1 - b_3) \times \frac{\lambda_3 - \lambda_2}{\lambda_3 - \lambda_1}$$
- MCI (maximum chlorophyll index) [3]
  - With b1 = 679 nm, b2 = 699 nm and b3 = 749 nm
  $$MCI = b_2 - b_3 + (b_1 - b_3) \times \frac{\lambda_3 - \lambda_2}{\lambda_3 - \lambda_1}$$
- FAI (floating algae index) [4]
  - With b1 = 641 nm, b2 = 855 nm and b3 = 1240 nm
  $$FAI = b_2 - b_1 + (b_3 - b_1) \times \frac{\lambda_2 - \lambda_1}{\lambda_3 - \lambda_1}$$

Figure 2. Indexes used for PRISMA images analysis.

Results

(1) Dornier. Study area: Adventfjorden bay (fig 2., area #1).

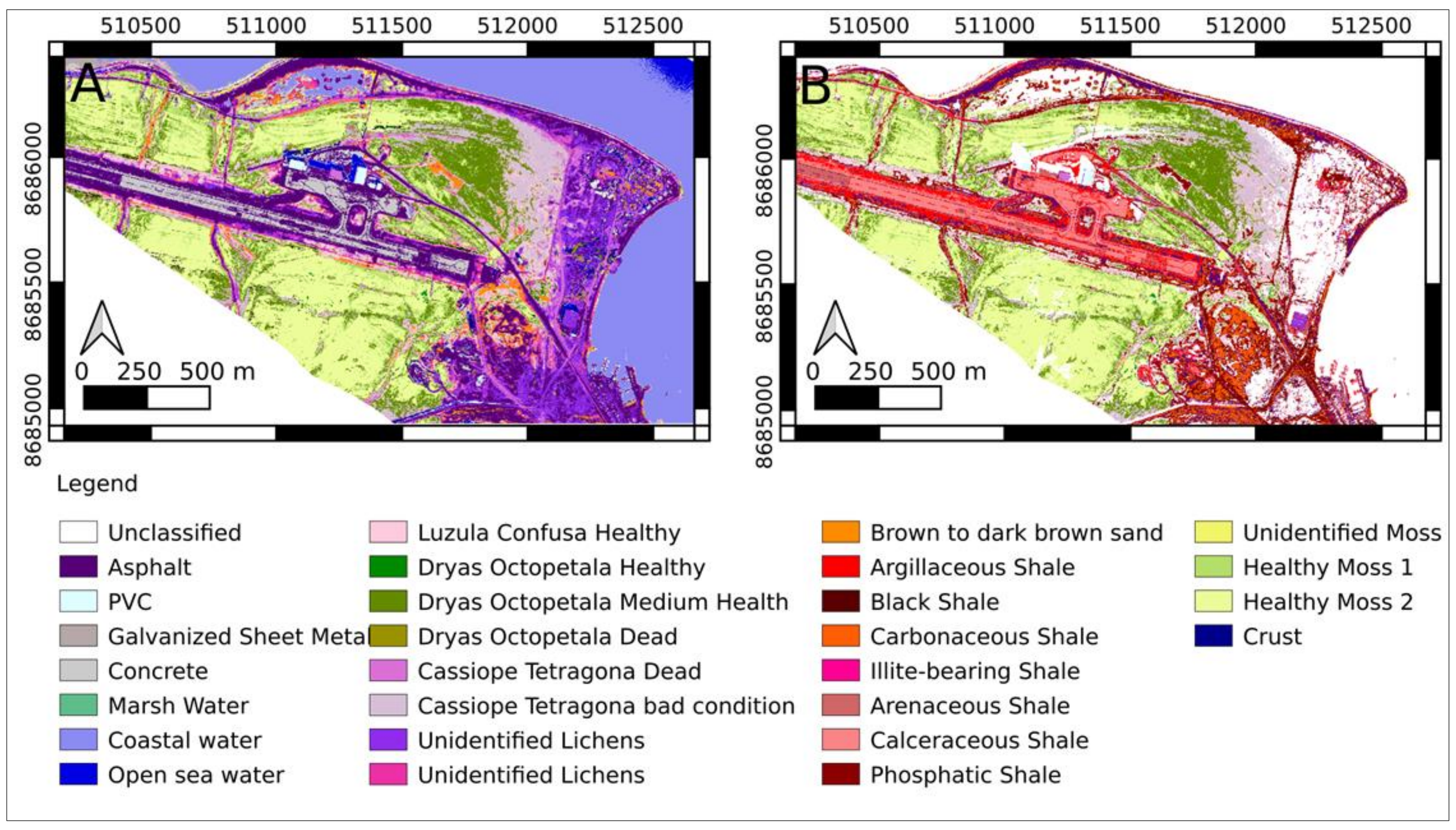

Figure 3. Dornier maps of classes from SAM endmember classification of SIOS-InfraNor dataset. A: limited set of endmembers and no restriction on the classifier; B: Shale endmembers included and a restriction imposed of the maximum angle at which the SAM is allowed to assign a pixel to the particular class.

(2) PRISMA | Study area: Grønfjorden (fig 2., area #3).

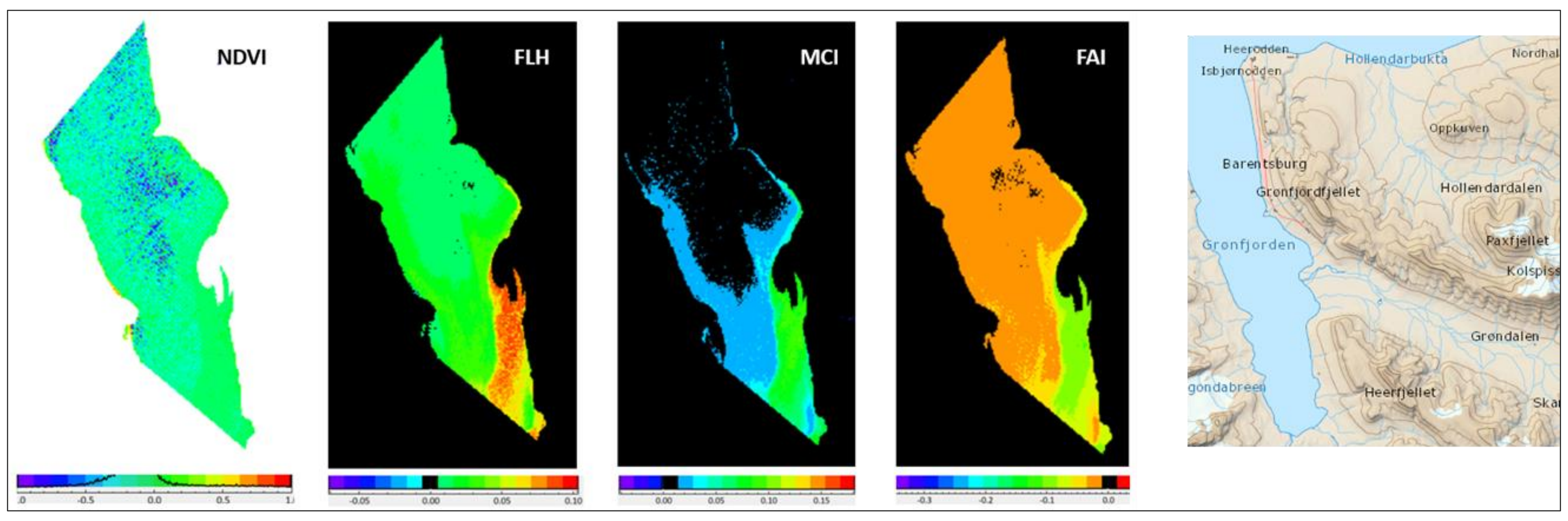

Figure 4: Indexes calculated; (a) NDVI, (b) FLH, (c) MCI, and (d) FAI. A plume is visible both in the original RGB image, as well as for the indices FLH, MCI and FAI. The plume comes from Grøndalselva in Grøndalen, and most likely carries sediments and brings them out into the fjord. The plume is not visible with NDVI, however, which can indicate that there is not much vegetation/chlorophyll in the plume. The FAI is also negative, indicating no floating algae in the area.

Conclusions

- The Dornier results could be improved by using dimensionality reduction followed by accuracy assessment.
- Hyperspectral imaging has potential to map ocean water properties in a RS manner.
- Ground truthing is fundamental for ocean colour mapping and chlorophyll estimation.
- The indexes resulted in different index-values, which might result in different concentrations for a certain region.
- Sensor calibration and corrections for atmospheric influences must be considered and improved.

Acknowledgements

This work wouldn't have been possible without the support of SIOS, ISP and HySpex. Many thanks to the lecturers who shared their knowledge and their projects during the SIOS training course.

References

- Bernstein, et al., 2012.Optical Engineering 51, No. 11 (2012): 111719-1 to 111719-11.
- Gower et al., (2005). https://doi.org/10.1080/01431160500075857
- Harris Geospatial 2020a. https://www.l3harrisgeospatial.com/docs/backgroundquac.html
- Harris Geospatial, 2020b. https://www.l3harrisgeospatial.com/docs/spectralanglemapper.html
- Hu, C. (2009). https://doi.org/10.1016/j.rse.2009.05.012
- IOCCG. (2014). Reports of the International Ocean-Colour Coordinating Group, 15.
- Kokaly et al., 2017, USGS Spectral Library Version 7: U.S. /ds1035.
- Kruse et al., 1993." Remote Sensing of Environment 44 (1993): 145-163.
- Letelier et al., (1996). Remote Sensing of Environment, 58(2), 215–223.
- Meerdink et al., 2019 https://doi.org/10.3133OSTRESS
- SIOS. 2019. https://sios-svalbard.org/aerialRSplatforms) [access: 20.10.2021]
- SISpec 2021. https://niveos.cnr.it/SISpec/ [access: 20.10.2021]
- Szymański et al., 2019. https:// doi.org/10.1017/S0032247419000251
- Thomson et al., 2021. https://doi.org/10.1088/1748-9326/abf464